NOVEL EXPERIMENTAL METHODS FOR THE GENERATION AND MULTI-MODALITY QUANTIFICATION OF MYOCARDIAL INFARCTION

Ph.D. Thesis Summary
by
Ákos Varga-Szemes, M.D.

Head of the Doctoral School: Sámuel Komoly, M.D., Ph.D., D.Sc.
Head of the Doctoral Program: Ákos Koller, M.D., Ph.D., D.Sc.
Supervisor: Tamás Simor, M.D., Ph.D.

Heart Institute, University of Pécs
Pécs
2013

1. INTRODUCTION

Cardiovascular disease is the number one cause of death in the Western World. Early reperfusion therapy is the most important aim in the treatment of acute myocardial infarct (MI). Universal achievement of this purpose, however, is almost impossible. Based on the assumed number of cardiac patients worldwide, generating a model for such situations is of major importance in the development and preclinical testing of new diagnostic and therapeutic strategies for patients missing the appropriate timeframe for revascularization following acute MI. As most of the available models have some limitations, an easily applicable, cost effective, MRI compatible, non-reperfused MI model is highly desirable.

The diagnosis of MI is usually based on the patient's physical status, ECG, the level of cardiac enzymes in the blood, and a coronary angiogram. Numerous additional imaging methods are available to confirm the diagnosis, evaluate, and quantify the myocardial damage, and monitor left ventricular (LV) recovery. Late Gadolinium (Gd) Enhancement Magnetic Resonance Imaging (LGE-MRI), however, has become the gold standard modality for the assessment of myocardial viability. Nevertheless, Gd-chelates can also be detected by X-ray based techniques. For instance, Coronary CT Angiography (CTA), a well-established diagnostic tool for the non-invasive evaluation of coronary artery disease, has been validated using Gd-enhanced Multi-detector CT (Gd-MDCT). Since the LGE-MRI phenomenon is based on the accumulation of Gd in the MI, it can be hypothesized that the LGE phenomenon can also be observed by CT due to the fact that CT detects Gd. Thus Gd-enhanced CTA, supplemented with the LGE protocol, could evaluate coronary status and myocardial viability noninvasively in a single imaging session in certain patients.

2. OBJECTIVES

The overall goal of our study was to develop a reliable and MRI compatible method for the generation of non-reperfused MI, and to investigate the feasibility of Gd-MDCT for the detection and quantification of MI.

2.1 Myocardial infarct model development

Our aim has been (1) the development of a percutaneous technique for the generation of non-reperfused MI; (2) the investigation of the MRI compatibility of the novel model; (3) and the confirmation of the non-reperfused nature of the model by histopathology.

2.2 Development of a Gadolinium based infarct quantification tool

We aimed (1) to develop an ex vivo heart model suitable for the performance of multi-modality imaging; (2) to investigate the ability of Gd-MDCT for the detection of MI; (3) to study the feasibility of Gd-MDCT for the quantification of MI; (4) to investigate the accuracy of the different MRI quantification methods for the evaluation of MI; and (5) to compare the accuracy of each method to the reference Triphenyl-Tetrazolium-Chloride (TTC) technique.

3. EMBOZENE™ MICROSPHERES INDUCED NON-REPERFUSED MYOCARDIAL INFARCTION IN AN EXPERIMENTAL SWINE MODEL

3.1 Introduction

Several animal species have been used to model MI, it, however, has been proven that the anatomy of the pig heart and its coronary circulation are the closest to those of humans. Creating closed-chest, non-reperfused MI model requires special techniques and/or materials that allow advancing and leaving an item or substance in the coronary artery providing direct or indirect mechanical obstruction and usually consequent thrombus formation. Several techniques have been developed to model non-reperfused MI, e.g., inflatable-detachable balloon occlusion; flexible plug, open-cell sponge, tungsten spiral, agarose gel bead, and microsphere (42μm) embolization; ethanol, thrombin, and n-butyl cyanoacrylate (n-BCA) injection. As many of those techniques have some shortcoming, in this work we introduce a new, easily applicable, cost effective, MRI compatible non-reperfused MI model in pigs using percutaneously administered Embozene microspheres.

3.2 Materials and Methods

3.2.1 Embozene preparation

Color advanced 900μm diameter Embozene™ microspheres were purchased in 1ml syringes. Embozene was mixed with 7.0ml iohexol to make the solution visible under fluoroscopy.

3.2.2 Myocardial infarct model

Anesthesia was initiated in male swine (n=31). The right femoral artery was surgically prepared and cannulated. A 6F coronary guide catheter was introduced to cannulate the ostium of the left main, an initial coronary angiography was performed, and then a microcatheter was introduced over a coronary guide wire into the Left Anterior Descending (LAD) or the Left Circumflex (LCX) coronary arteries. After determining the proper position for the occlusion using the radiopaque tip of the microcatheter, the Embozene mixture was flushed into the coronary artery under fluoroscopic control. When the lumen of the coronary artery distal to the tip of the microcatheter was completely filled with Embozene, the injection was stopped and the occlusion was confirmed by repeated angiography.Then the microcatheter was removed and the femoral artery was decannulated, surgically ligated, and the wound was closed.

3.2.3 Magnetic Resonance Imaging

MRI studies were carried out using a 1.5T GE Signa-Horizon scanner. Pigs were anesthetized and ventilated mechanically. Imaging was performed during breath-hold at end-inspiration. Following cine and T_2-weighted imaging, a bolus of 0.2mmol/kg Gd-DTPA was administered as contrast agent (CA). T_1-weighted inversion recovery (IR), short-axis oriented images were generated to assess viability. At the end of their planned in vivo MRI session (2, 4, 14, and 56 days following MI generation), animals were sacrificed.

3.2.4 Image analysis

Localization of MI was assessed using the standardized 17-segment model. Visual assessment of the quality of the MRI images was performed to study possible occurrence of image artifacts caused by the administered microspheres.

3.2.5 Triphenyl-Tetrazolium-Chloride staining

TTC staining was used as a post-mortem gold standard to confirm the existence of MI. Hearts were bread-sliced, and subsequently the slices were incubated for 20 min with a buffered 1.5% TTC solution at a temperature of 37°C.

3.2.6 Microscopic histology

Tissue samples were prepared from the infarct, peri-infarct, and healthy myocardial regions. The samples were fixed in 10% formalin, embedded in paraffin, sectioned at 5μm thickness, and stained with H&E and Masson's Trichrome.

3.3 Results

Microsphere administration was successfully applied in all 31 pigs. Seven animals were excluded from the study (five of them died during the observation period and two of them died in the cage). Twenty-four animals reached their planned study endpoint, resulting in a mortality rate of 22.6%.

In eleven pigs the LAD, and in thirteen other pigs the LCX, was occluded. During the observation period arrhythmia was observed in nine of the surviving animals: isolated premature ventricular complexes and/or short ventricular tachycardias in seven cases, 2^{nd} degree atrioventricular block in one pig, and ventricular fibrillation after repeated episodes of ventricular tachycardia in one case.

Except a single animal, reflux of the microspheres to any non-target vessel was not observed on fluoroscopy and no MI in unexpected territories in the LV was detected by MRI or by TTC. Existence of MI was confirmed in the different phases with in vivo MRI, macroscopic pathology and histology. The MI localizations determined by MRI and TTC corresponded with the territories supplied by the target vessels. No artifacts with significant influence on image assessment were observed.

3.4 Discussion

In this study, we reported the use of percutaneously administered Embozene microspheres to generate non-reperfused MI in a swine model. The mortality rate in this study was similar to other authors' experiences with coil embolization models.

The procedure can be easily controlled under fluoroscopy since the microspheres are diluted in iodine contrast material (CM). The administration, however, requires some experience. The procedure requires slow injection while the syringe is kept in a horizontal position, providing constant rate of distribution of the microspheres. The injection becomes increasingly harder when the coronary artery is being filled with microspheres, indicating that the anterograde flow in the artery is being significantly reduced. At this point, the artery is

temporarily outlined by the entrapped iodine contrast under the fluoroscopy and the occlusion can be confirmed by angiography.

While open chest MI models have some benefits, these models also have many limitations. The increased length of the procedure, the higher mortality rate, the high occurrence of complications due to the thoracotomy, issues with MRI compatibility etc., have motivated the development of closed chest techniques. Some of these techniques, mentioned in the Introduction, have significant limitations. The inflatable, detachable balloons have been removed from the U.S. market since safety issues were reported. Introduction of large items, such as flexible plugs or sponges, requires cannulation of the carotid artery. Administration of liquids may cause accidental embolization into non-target vessels due to the reflux of the agents. Among the techniques available to date, tungsten spiral embolization seems to be a promising method. Tungsten spirals are MRI safe, but the MRI compatibility of tungsten-containing materials regarding artifacts, however, is not clear. Using the microsphere embolization technique, the MRI image quality was not influenced either, and the assessment of T_1- and T_2-weighted images did not show any artifacts interfering with MI visualization.

The methods for MI generation described above can be classified into two well defined approaches: (1) advancing a solid material into the coronary artery to create immediate occlusion or induce thrombus formation, or (2) flushing a liquid into the coronary artery generating tissue changes, thrombus formation, and consequent occlusion. Our method introduced here could be considered a mixture of both. Embozene microspheres can be easily injected as a liquid through a delivery catheter of the proper size, using a 6F sheath inserted in the femoral artery. The size of the microspheres provides a plug-like occlusion. As a result, the column of microspheres stays in place at the site of administration for up to at least 54 days.

This method has advantages and also possible shortcomings compared to the other available techniques. The main advantages of Embozene microsphere embolization are the easy applicability, the cost effectiveness, and the MRI compatibility. The administration, however, requires some experience, and the level of occlusion differs from that of the other techniques.

Liquids, such as n-BCA or ethanol, reach the microvascular level of the coronary artery circulation, while plugs or coils cause an occlusion at the level of placement. Embozene microspheres work similarly to the latter as they get trapped in the target artery at the level of ~900µm diameter and they fill the artery as a pearl necklace up to right below the place of administration. It is clear that the place of occlusion is not as well defined as with, e.g., coil embolization. The occlusion, however, does not reach the microvascular level, but rather affects the epicardial level of the coronary circulation.

4. DETERMINATION OF INFARCT SIZE IN EX VIVO SWINE HEARTS BY MULTI-DETECTOR COMPUTED TOMOGRAPHY USING GADOLINIUM AS CONTRAST MEDIUM

4.1 Introduction

The first use of Gd-chelates as radiographic CM was reported in 1989. Since then, several cases using Gd-chelates in various radiographic procedures have been published. Furuichi et al. reported the use of Gd-DTPA, in the course of percutaneous coronary intervention. Gupta et al. studied the thoracic aorta, and cervical and abdominal vessels, by 3D CTA using Gd-DTPA and found sufficient contrast to clearly define these vessels. Kälsch et al. studied 19 patients with contraindication to iodinated CM and found reduced but acceptable image quality for diagnostic purposes using Gd-based CM in coronary angiography. A review article by Strunk et al. on the use of Gd-DTPA for non-MRI applications concludes that Gd-based CM could be safely used for radiography. It is, however, presently approved for MRI use only.

Using CT with Gd as CM for the detection or quantification of MI has not yet been reported. The aim of this ex vivo study was to investigate the ability of MDCT using Gd-DTPA as CM (Gd-MDCT) to evaluate MI, and compare the results with data obtained by the gold standard LGE-MRI and the ex-vivo gold standard TTC staining method.

4.2 Materials and methods

4.2.1 Experimental model

MI was generated in six male swine under Isoflurane anesthesia by a 90-minute long percutaneous balloon occlusion of the LAD coronary artery. Reperfusion of the coronary artery was confirmed by repeated angiography. One week later, the animals received 0.2mmol/kg Gd-DTPA by bolus injection and were sacrificed 20 minutes later. Excised hearts were embedded in 4.2% agar gel providing a stable position for the heart structures during the imaging sessions.

4.2.2 Multi-Detector Computed Tomography

MDCT studies were carried using a Philips Brilliance 64 scanner. Images were collected covering the entire heart using a tube voltage of 80, 120, or 140kV.

4.2.3 Magnetic Resonance Imaging

MRI acquisitions were conducted using a 1.5T GE Signa-Horizon scanner. Using an IR pulse sequence, multi-slice short axis oriented LGE images were acquired covering the entire heart.

4.2.4 Triphenyl-Tetrazolium-Chloride staining

Following the imaging sessions, hearts were frozen and bread-sliced, based on the orientations of the tomographic slices. Subsequently, the slices were incubated for 20min with a buffered 1.5% TTC solution at 37°C.

4.2.5 Histopathology

Tissue samples were prepared to confirm the existence of MI by microscopic histopathology. The samples were fixed in 10% formalin, embedded in paraffin, sectioned at 5μm thickness, and stained with H&E.

4.2.6 Image analysis

MDCT and MRI dicom images were evaluated using ImageJ v1.42. The mean MRI signal intensity (SI) or CT attenuation of the remote and the infarcted myocardium, as well as the mean SI of the background noise were measured with multiple regions of interest.

To compare the image quality provided by MDCT vs. MRI, the signal to noise ratio (SNR), contrast to noise ratio (CNR), and signal intensity ratio (SIR) were calculated.

For further analysis, the endocardial and epicardial contours of the LV were traced and the total LV myocardial volume was calculated (LVV). The thresholding technique was used to delineate MI. Mean SI of the remote plus 2, 3, 4, 5 and 6 times the standard deviation (SD), and the full-width at half-maximum (FWHM) method were used to define the threshold limit in the MRI images. For MDCT images, mean attenuation of the remote areas plus two times the SD was used to threshold the images. The total infarct volume of each heart (IV) was calculated and expressed as a percentage (Infarct Fraction, IF) of the LVV.

4.2.7 Statistical analysis

Statistical analysis was carried out using SigmaStat v2.03. Data were expressed as mean±SD. One-way analysis of variance (ANOVA) was used to compare results among the imaging methods and the TTC-staining. Bland-Altman plots were used to analyze the accuracy of each technique. Comparison of CNR, SNR, and SIR among the different MDCT settings and MRI was carried out using one-way ANOVA. *P*-value <0.05 was interpreted to indicate a significant difference.

4.3 Results

All three techniques provided sufficient image quality to visualize MI. Microscopic evaluation of the tissue samples confirmed the existence of MI. The average attenuation, SI, the calculated SNR, CNR, and SIR values are shown in Table 1.

Comparing the MDCT images obtained by the three different kV settings, the mean of the background air and the remote myocardium showed statistically the same average attenuation independently of tube voltage. The SD of the remote myocardium (i.e. the noise of the remote areas) showed a strong linear relationship (R^2=0.9999) with $(kV)^{-1.3}$. The background noise showed a similar correlation (R^2=0.9786). Mean MI attenuation values at 80kV were significantly higher (P<0.01) than at 120 or 140kV, while no statistical difference was observed between the latter two. SNR_{remote} was significantly lower at 80kV (P<0.05) than at the other two tube voltages, while no difference was observed between 120 and 140kV. There was no statistical difference among the $SNR_{infarct}$, CNR and SIR values measured at the different kV settings. All these ratios were significantly lower than ratios measured by MRI (P<0.001, power of 0.902).

Table 1 Average attenuation (HU) and SI (arbitrary units, au) values, and calculated SNR, CNR and SIR in MDCT and MRI images, respectively (mean±SD, n=6)

	MDCT			MRI	*P*-value MDCT vs. MRI
	80kV	120kV	140kV		
Background	-1009±2.5	-1010±2.1	-1009±2.6	144±10.2	
Remote	43±1.9	42±1.9	42±2.0	168±12.5	
Remote SD	16±0.9	8±0.5	6±0.5	16±4.2	
Infarct	91±6.2	81±5.1	80±5.0	734±118.1	
Infarct peak	133±16.1	109±12.3	100±5.4	921±42.4	
SNR remote	4.0±0.3	4.5±0.6	4.6±0.5	10.7+4.5	<0.05
SNR infarct	8.5±1.0	8.8±1.1	8.8±1.2	46.9+11.2	<0.05
CNR	4.5±0.7	4.3±0.8	4.2±0.7	36.2+6.1	<0.05
SIR	2.1±0.2	1.9±0.1	1.9±0.1	4.4+0.7	<0.05

Average LVV, IV and IF values measured by MDCT, MRI and TTC are shown in Table 2. Average LVVs obtained by the different techniques were in good agreement (*P*=N.S.).

Table 2 Average LVV, IV, and IF (%) values (mean±SD, n=6) measured by each technique.

Modality	Tube voltage (kV)	LVV (ml)	IV (ml)	IF (%)
MDCT	80	72.06±13.23*	1.65±1.24	2.34±2.11
	120		3.80±1.78	5.36±2.01
	140		5.06±1.64	7.15±2.28
	Threshold			
MRI	2SD	74.72±13.15*	8.91±2.99	12.03±3.81
	3SD		8.07±1.15	10.80±1.89
	4SD		7.22±1.31	9.66±1.49
	5SD		5.87±1.26	7.86±2.03
	6SD		5.47±1.23	7.36±1.57
	FWHM		4.36±1.16	5.86±1.55
TTC		75.42±14.85	5.36±1.57	7.34±2.30

*The LV volume was calculated only once with each method, since the same endo- and epicardial contours were used for each kV (MDCT) or threshold (MRI)

The multiple comparison method showed that $MDCT_{80kV}$, LGE-MRI with 2 and 3SD thresholds are significantly different from the reference TTC (P<0.05), while no statistical difference was observed among IVs and IFs obtained by $MDCT_{120kV}$, $MDCT_{140kV}$, MRI_{4SD}, MRI_{5SD}, $MRI_{6SD,}$ MRI_{FWHM} and TTC (Figure 1).

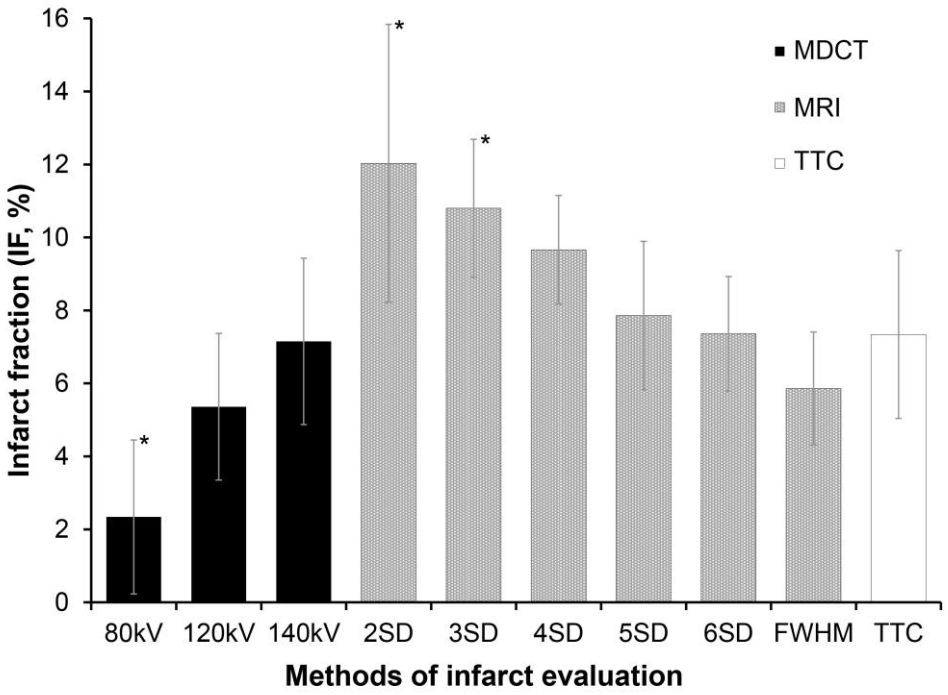

Figure 1

Bland-Altman plots indicate good agreement for the IF values obtained by $MDCT_{120kV}$, $MDCT_{140kV}$, MRI_{5SD}, MRI_{6SD} and MRI_{FWHM} vs. the gold standard TTC method. Note, that the mean of differences is less than 1% in the case of $MDCT_{140kV}$ and MRI_{6SD} (Figure 2), and less than 2% with $MDCT_{120kV}$, MRI_{5SD} and MRI_{FWHM}. The Bland-Altman analysis of $MDCT_{80kV}$ showed a bias of -5.07% (~3.7ml) indicating a significant underestimation of the IF by this method. Plots of the MRI data with 2 and 3SD thresholding showed overestimation of the IF with a bias of 4.68% (~3.41ml) and 3.50% (~2.61ml), respectively.

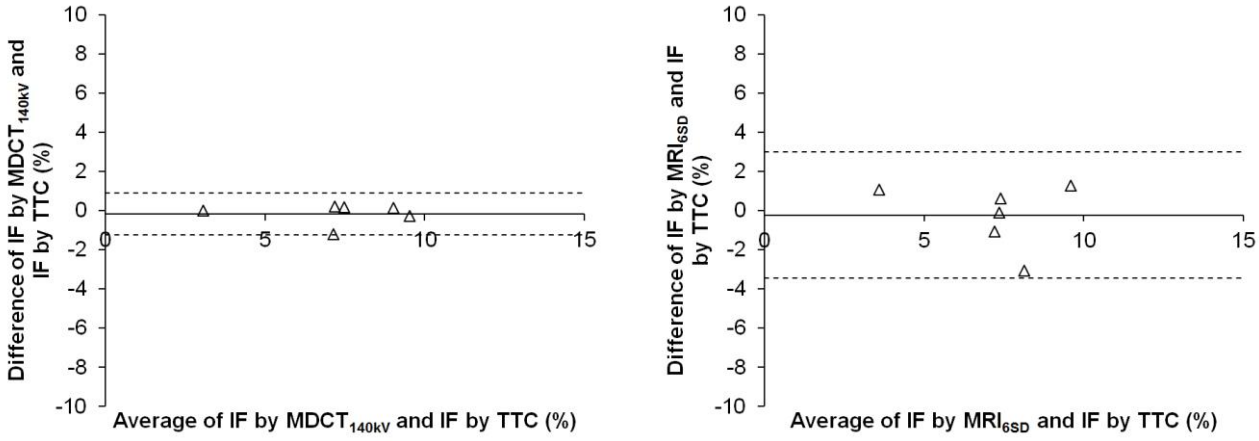

Figure 2

4.4 Discussion

We have demonstrated in an ex-vivo experimental model that quantification of MI using the Gd-MDCT technique is feasible, providing accurate evaluation of MI size. We have also demonstrated that the agar embedded ex-vivo heart model is suitable for the performance of repeated, or multi-modality, imaging.

The SNR, CNR, and SIR results were in good agreement with other investigators' in-vivo findings. Measurement of these parameters in infarcted myocardium by Gd-MDCT showed that all three parameters were significantly lower than those obtained from LGE-MRI.

The MI was visually detectable by Gd-MDCT at all settings. The measured MI size, however, depended on the tube voltage used. The noise in the remote myocardium influenced the accuracy of the MI quantification because the thresholding level depended on the myocardial noise. In this study, we found that MI size measured by Gd-MDCT at 140kV showed good correlation with the reference TTC. Applying 80kV tube voltage, however, underestimated MI size. This finding can be explained by the fact, that the noise of the remote myocardium is increased at lower tube voltages.

In our study, the LGE-MRI method, using the higher 5 or 6SD thresholds, provided accurate determination of MI. LGE-MRI using higher threshold limits overestimated the MI size. The reason for MI overestimation using LGE may be due to the partial volume effects mostly presenting in the patchy peripheral zone of the MI.

Our finding that Gd-MDCT at high tube voltage with 2SD thresholding yielded more accurate results than LGE-MRI with the same thresholding, may be due to several reasons. The spatial resolution of MDCT is higher than that of MRI. The voxel volume in our study was $0.1mm^3$ (MDCT) vs. $1.95mm^3$ (MRI), resulting in a negligible partial volume effect in MDCT, but not in MRI. Another reason is the difference between the mechanisms of the contrast effect of Gd-DTPA in these two imaging modalities. In MRI, Gd-chelates act as a *contrast agent*, since they exert an effect on the protons of the tissue water molecules, and this effect is observed as SI enhancement by MRI. SI enhancement induced by a Gd CA depends nonlinearly on the concentration of the CA in the myocardial voxel observed. In CT, Gd works as a *contrast medium*. The high atomic weight of Gd makes it radiopaque, thus its simple physical presence, and not an indirect effect on another molecule, is measured. Infarct determination by Gd-MDCT is straightforward since Gd concentration in any voxel is related to the attenuation in a linear fashion. The literature suggests that the diagnostic value of Gd-based CT techniques is inferior to the iodine based methods. Although it is evident that Gd-MDCT provides less contrast than Gd-MRI or iodine CT, our results, nevertheless, proved the presence of sufficient contrast for distinguishing between normal and infarcted myocardium using 0.2mmol/kg Gd-DTPA.

5. DISCUSSION

5.1 Myocardial infarct model development

In spite of the effort to provide revascularization therapy within a reasonable time for patients with acute MI, a significant number of MIs remain untreated. Thus generating an experimental model of the clinical scenario of non-treated MIs is of major importance. Since CMR has become the appropriate diagnostic tool in several cardiovascular indications, therefore an animal model should be MRI safe and MRI compatible. As the currently available techniques for the generation of non-reperfused MI raised many concerns regarding safety, reliability and MRI compatibility, the development of an easy and cost effective model suitable for MRI studies was highly desired.

In this study, we have introduced a novel animal model of non-reperfused MI. The percutaneously administered Embozene microsphere technique we used in the swine model can be easily controlled under fluoroscopy. The non-reperfused nature of the model has been confirmed at the end of the infarct generation procedure by repeated coronary angiography, as well as at 2, 4, 14, or 56 days following infarct generation by histopathology.

The main advantages of our microsphere embolization method are the easy applicability and the cost effectiveness. The only method reported in the literature having comparable reliability is coil embolization. The MRI compatibility of coils and spirals advanced into the coronary artery, however, is still a question. Since our procedure avoids the placement of any metallic material in the coronary artery, it can be considered MRI safe and compatible, as proven in a relatively large number of our MRI experiments.

5.2 Development of a Gadolinium based infarct quantification tool

In this study we reported the development of an agar embedded ex-vivo heart model of MI that is suitable for the performance of repeated, or multi-modality, imaging, as well as for the co-registration of imaging methods with each other and with gross pathology. Employing this model we demonstrated the feasibility of quantification of MI by the MDCT technique using Gd as CM. Based on our experiments, MI size measured by Gd-MDCT at 140kV showed the best correlation with the reference TTC.

Presently, the applicability of Gd-MDCT in the clinical diagnosis of MI is theoretical only. Initially, further studies will be required to evaluate the feasibility of this method to detect MI in *in vivo* circumstances. Furthermore, the safety of Gd contrast materials has to be clarified, especially in patients with severe renal impairment who may develop NSF due to the de-chelation of the less stable linear chelates. Since cyclic Gd chelates have extremely high stability, those compounds may have a better chance to get approval for such off label use.

For experimental purposes, Gd-MDCT is capable to determine the concentration of Gd accumulated in a specific volume element. The Gd-MDCT method combined with LGE-MRI may be feasible to correlate the Gd concentration (as reflected in CT density) and the relaxation rate (as MRI R_1) in any tissue accumulating Gd (e.g. MI, tumors), providing an independent tool for the validation of Gd contrast enhanced MRI results.

6. CONCLUSIONS

We have demonstrated the feasibility of the generation of MI using Embozene microspheres and the MRI compatibility of this method. Our method can be used as an alternative technique to induce non-reperfused MI.

We have also demonstrated the feasibility of the Gd-MDCT technique for the evaluation of MI, at least in an ex-vivo experimental setting. Gd-MDCT is able to quantify MI with the same accuracy as the ex vivo gold standard does.

7. NOVEL FINDINGS

1. We have worked out a novel, cost effective, percutaneous technique for the generation of non-reperfused MI.
2. We have proven in a large number of MRI experiments that our novel infarct generation method is fully suitable for MRI studies.
3. We have also proven by postmortem histopathology that Embozene microspheres create total occlusion in the target vessel and initiate consequent thrombosis. The occlusion is reliably maintained up to 56 days after the induction of MI.
4. We have developed an ex vivo method, the agar embedded heart model, that is suitable for the performance of repeated and/or multi-modality imaging, when a stable position of the sample is required.
5. We have demonstrated that MDCT enhanced by Gd-DTPA, an MRI contrast agent, is able to detect MI.
6. We have also demonstrated that Gd-MDCT, performed with appropriate settings, provides the accurate assessment of MI.
7. We have found that Gd-MDCT provides the same accurate evaluation of MI as the in vivo gold standard LGE-MRI (with appropriate post-processing) and the ex vivo gold standard TTC staining do.

8. PUBLICATIONS OF THE AUTHOR

8.1 Peer reviewed original research publications related to the thesis

1. Varga-Szemes A, Kiss P, Brott BC, Wang D, Simor T, Elgavish GA: Embozene™ Microspheres Induced Non-reperfused Myocardial Infarction in an Experimental Swine Model. Catheter Cariovasc Interv 2013;81(4):689-97 **IF: 2.398**

2. Varga-Szemes A, Ruzsics B, Kirschner R, Singh SP, Kiss P, Brott BC, Simor T, Elgavish A, Elgavish GA: Determination of Infarct Size in Ex Vivo Swine Hearts by Multi-detector Computed Tomography Using Gadolinium as Contrast Medium. Invest Radiol 2012;47(5):277-283 **IF: 4.665**

8.2 Peer reviewed abstracts related to the thesis

1. Varga-Szemes A, Ruzsics B, Kirschner R, Singh SP, Simor T, Elgavish A, Elgavish GA: Determination of Infarct Size In Ex Vivo Swine Hearts Using Gadolinium-Enhanced Multi-Detector Computed Tomography. J Cardiovasc Comput Tomogr 2010;45:S53. 5th Annual Scientific Meeting of the Society of Cardiovascular Computed Tomography, 2010, Las Vegas, NV, USA

2. Varga-Szemes A, Ruzsics B, Kirschner R, Singh SP, Simor T, Elgavish A, Elgavish GA: Gadolinium-Enhanced Multi-Detector Computed Tomography for the Evaluation of Myocardial Infarct. 38th Annual Meeting of the North American Society for Cardiovascular Imaging, 2010, Seattle, WA, USA

3. Varga-Szemes A, Kiss P, Brott BC, Simor T, Elgavish GA: Embozene microspheres for the generation of non-reperfused myocardial infarction. 39th Annual Meeting of the North American Society for Cardiovascular Imaging, 2011, Baltimore, MD, USA

8.3 Original peer reviewed publications not related to the thesis

1. Faludi R, Toth L, Komocsi A, Varga-Szemes A, Simor T, Papp L: Chronic Postinfarction Pseudo-pseudoaneurysm Diagnosed by Cardiac MRI. J Magn Reson Imaging 2007;26:1656-1658

2. Kirschner R, Toth L, Varga-Szemes A, Simor T, Suranyi P, Ruzsics B, Kiss P, Toth A, Baker R, Brott BC, Litovsky S, Elgavish A, Elgavish GA: Differentiation of Acute and Four-week Old Myocardial Infarct with Gd(ABE-DTTA)-enhanced CMR. J Cardiovasc Magn Reson 2010;12:22

3. Simor T, Suranyi P, Ruzsics B, Toth A, Toth L, Kiss P, Brott BC, Varga-Szemes A, Elgavish A, Elgavish GA: Percent Infarct Mapping for Delayed Contrast Enhancement MR Imaging to Quantify Myocardial Viability by Gd(DTPA). J Magn Reson Imaging 2010;32:859-868

4. Kirschner R, Varga-Szemes A, Simor T, Suranyi P, Kiss P, Ruzsics B, Brott BC, Elgavish A, Elgavish GA: Acute Infarct Selective MRI Contrast Agent. Int J Cardiovasc Imaging 2012;28(2):285-93

5. Kirschner R, Varga-Szemes A, Brott BC, Litovsky S, Elgavish A, Elgavish GA, Simor T: Quantification of myocardial viability distribution with Gd(DTPA) bolus-enhanced, signal intensity-based percent infarct mapping. Magn Reson Imaging 2011;29(5):650-8

8.4 Peer reviewed abstracts not related to the thesis

1. Toth L, Faludi R, Fodi E, Knausz M, Varga-Szemes A, Papp L, Simor T: Evidence Based, MRI Strengthened Risk Stratification Strategy for Hypertrophic Cardiomyopathy Patients – A Follow

Up Study. Eur J Echocardiogr 2006;7:S205. 10th Annual Meeting of the European Association of Echocardiography, 2006, Prague, Czech Republic

2. Toth L, Faludi R, Fodi E, Knausz M, Varga-Szemes A, Repa I, Papp L, Simor T: Cardiac MRI for the Assessment of Risk of Sudden Cardiac Death in Patients with Hypertrophic Cardiomyopathy. Abstract Book p136. 5th Annual Meeting of the European Society of Cardiology Working Group on Cardiovascular Magnetic Resonance Imaging, 2006, Vienna, Austria
3. Toth L, Varga-Szemes A, Faludi R, Toth A, Papp L, Simor T: MRI Study in Isolated Left Ventricular Noncompaction. J Magn Reson Imaging 2007;9:406-407. 10th Annual Meeting of the Society for Cardiovascular Magnetic Resonance, 2007, Rome, Italy
4. Varga-Szemes A, Toth L, Faludi R, Toth A, Repa I, Papp L, Simor T: MRI Study in Isolated Left Ventricular Noncompaction. Cardiologia Hungarica 2007;37:A72. Scientific Congress of the Hungarian Society of Cardiology, 2007, Balatonfured, Hungary
5. Toth L, Horvath I, Varga-Szemes A, Kantor M, Repa I, Papp L, Simor T: MRI Measurement of Infarct Size in Patients with Chronic Coronary Occlusion. Cardiologia Hungarica 2007;37:A52. Scientific Congress of the Hungarian Society of Cardiology, 2007, Balatonfured, Hungary
6. Toth L, Faludi R, Toth A, Varga-Szemes A, Repa I, Papp L, Simor T: Correlation of the Extent of Left Ventricular Noncompaction and Left Ventricular Function. Eur J Heart Failure 2007;6:S161. Heart Failure Congress, 2007, Hamburg, Germany
7. Varga-Szemes A, Toth L, Faludi R, Papp L, Simor T: Assessment of ECG Abnormalities in Patients with Isolated Left Ventricular Noncompaction. Cardiologia Hungarica 2007;37:C3. 6th Congress of the Hungarian Society of Cardiology Working Group on Arrhythmia, 2007, Szeged, Hungary
8. Toth L, Varga-Szemes A, Faludi R, Sepp R, Nagy V, Repa I, Varga A, Forster T, Papp L, Simor T: Which are the Determinant Factors Altering Left Ventricular Function and Clinical Outcome of Patients with Isolated Noncompact Cardiomyopathy? Eur J Echocardiogr 2007;8:S165. 11th Annual Meeting of the European Association of Echocardiography, 2007, Lisbon, Portugal
9. Varga-Szemes A, Toth L, Faludi R, Papp L, Simor T: Characterization of Left Ventricular Regional Function in Isolated Left Ventricular Noncompaction. Cardiologia Hungarica 2008;38:B7 Scientific Congress of the Hungarian Society of Cardiology, 2008, Balatonfured, Hungary
10. Manfai B, Faludi R, Rausch P, Tahin T, Fodi E, Toth L, Varga-Szemes A, Papp L, Simor T: Reverse-remodeling of the Left Atrium After Catheter Ablation of Atrial Fibrillation. Cardiologia Hungarica 2008;38:B43 Scientific Congress of the Hungarian Society of Cardiology, 2008, Balatonfured, Hungary
11. Varga-Szemes A, Toth L, Faludi R, Papp L, Simor T: Novel Parameter for the Evaluation of Left Ventricular Noncompaction. Abstract CD #54. 6th Annual Meeting of the European Society of Cardiology Working Group on Cardiovascular Magnetic Resonance Imaging, 2008, Lisbon, Portugal
12. Kantor M, Toth L, Varga-Szemes A, Horvath I, Papp L, Simor T: The Relationship Between of the Extent of Myocardial Infarction and Global Cardiac Function in Chronic Total Occlusion in the Presence and Absence of Coronary Collateral Circulation. Abstract CD #35. 6th Annual Meeting of the European Society of Cardiology Working Group on Cardiovascular Magnetic Resonance Imaging, 2008, Lisbon, Portugal

13. Varga-Szemes A, Toth L, Faludi R, Papp L, Simor T: Assessment of Regional Left Ventricular Function in Isolated Left Ventricular Noncompaction. Eur J Heart Failure 2008;7:S33. Heart Failure Congress, 2008, Milan, Italy

14. Varga-Szemes A, Toth L, Faludi R, Papp L, Simor T: Assessment of ECG Abnormalities in Patients with Left Ventricular Noncompaction. Eur J Echocardiogr 2008;9:S96-97. 12th Annual Meeting of the European Association of Echocardiography, 2008, Lion, France

15. Faludi R, Toth L, Varga-Szemes A, Fodi E, Simor T: Correlations Between Systolic and Diastolic Function in a Group of Subjects with Variable Degrees of Left Ventricular Diastolic and Systolic Dysfunction. Eur J Heart Failure 2009;8:S1456. Heart Failure Congress, 2009, Nice, France

16. Kirschner R, Varga-Szemes A, Toth L, Simor T, Suranyi P, Ruzsics B, Kiss P, Toth A, Baker R, Brott BC, Litovsky S, Elgavish A, Elgavish GA: Reinfarction-Specific Magnetic Resonance Imaging Contrast Agent. J Am Coll Cardiol 2010;55:A84. 59th Annual Scientific Session of the American College of Cardiology, 2010, Atlanta, GA, USA

17. Singh SP, Varga-Szemes A, Goetze S, Nath H: Feasibility of combined adenosine augmented SPECT and MDCT for evaluation of myocardial perfusion and coronary artery morphology. J Cardiovasc Comput Tomogr 2010;45:S71. 5th Annual Scientific Meeting of the Society of Cardiovascular Computed Tomography, 2010, Las Vegas, NV, USA

18. Kirschner R, Varga-Szemes A, Toth L, Simor T, Suranyi P, Kiss P, Ruzsics B, Toth A, Brott BC, Elgavish A, Elgavish GA: Acute Infarct Selective MRI Contrast Agent. J Am Coll Cardiol 2010;56:B88. Transcatheter Cardiovascular Therapeutics Conference, 2010, Washington, DC, USA

19. Varga-Szemes A, Kirschner R, Toth L, Brott BC, Simor T, Elgavish A, Elgavish GA. In Vivo R1 Based Percent Infarct Mapping Using Continuous Gd(DTPA) Infusion Aided Magnetic Resonance Imaging. 38th Annual Meeting of the North American Society for Cardiovascular Imaging, 2010, Seattle, WA, USA

20. Singh SP, Varga-Szemes A, Goetze S, Nath H: Quantitative Evaluation of Myocardial Perfusion Abnormalities Using Adenosine Augmented MDCT and SPECT. 38th Annual Meeting of the North American Society for Cardiovascular Imaging, 2010, Seattle, WA, USA

21. Kirschner R, Varga-Szemes A, Toth L, Brott BC, Simor T, Elgavish A, Elgavish GA: Accurate Determining of Myocardial Viability Distribution with Percent Infarct Mapping. 38th Annual Meeting of the North American Society for Cardiovascular Imaging, 2010, Seattle, WA, USA

22. Kirschner R, Varga-Szemes A, Toth L, Brott BC, Simor T, Elgavish A, Elgavish GA: Acute Infarct Selective Magnetic Resonance Imaging Contrast Agent. 38th Annual Meeting of the North American Society for Cardiovascular Imaging, 2010, Seattle, WA, USA

23. Singh SP, Varga-Szemes A, Goetze S, Nath H: Feasibility of Combined Adenosine Augmented SPECT and MDCT for Evaluation of Myocardial Perfusion and Coronary Artery Morphology. Abstract# LL-CAS-TH2B. 96th Scientific Assembly and Annual Meeting of the Radiological Society of North America, 2010, Chicago, IL, USA

24. Pump A, Rausch P, Varga-Szemes A, Tahin T, Papp L, Simor T: Efficacy of Pulmonary Vein Isolation in Patients with Persistent Atrial Fibrillation. Cardiologia Hungarica 2010;37:C3. 7th Congress of the Hungarian Society of Cardiology Working Group on Arrhythmia, 2010, Budapest, Hungary

25. Pump A, Simor P, Rausch P, Varga-Szemes A, Tahin T, Papp L: Efficacy of pulmonary vein isolation for persistent atrial fibrillation regarding some specific parameters. J Cardiovasc Electrophysiol 2011;22:S105. 12th International Workshop on Cardiac Arrhythmias, 2011, Venice, Italy

26. Kirschner R, Varga-Szemes A, Simor T, Elgavish GA. Differentiation of myocardial infarct age using Gd(ABE-DTTA), an MRI contrast agent. Cardiologia Hungarica 2011;41:F57, Scientific Congress of the Hungarian Society of Cardiology, 2011, Balatonfured, Hungary

27. Kirschner R, Varga-Szemes A, Simor T, Brott BC, Litovsky S, Elgavish A, Elgavish GA: Quantification of infarct size and mixing of necrotic and viable myocardial tissue with signal intensity-based percent infarct mapping. Eur Heart J 2011;32:S46. Annual meeting of the European Society of Cardiology, 2011, Paris, France

28. Varga-Szemes A, Kirschner R, Brott BC, Simor T, Elgavish A, Elgavish GA: Percent Infarct Mapping for the evaluation of chronic myocardial infarction. 39th Annual Meeting of the North American Society for Cardiovascular Imaging, 2011, Baltimore, MD, USA

29. Varga-Szemes A, Kirschner R, Brott BC, Simor T, Elgavish A, Elgavish GA: Myocardial infarct density distribution by MRI. 40th Annual Meeting of the North American Society for Cardiovascular Imaging, 2012, Pasadena, CA, USA

30. Varga-Szemes A, Kirschner R, Brott BC, Simor T, Elgavish GA: Contrast uptake kinetics of microvascular obstruction in a reperfused and a non-reperfused acute infarct model. 40th Annual Meeting of the North American Society for Cardiovascular Imaging, 2012, Pasadena, CA, USA

9. ACKNOWLEDGEMENTS

First and foremost I would like to express my gratitude to my mentor, Dr. Tamás Simor, for his encouragement and support throughout my Ph.D. studies.

I would also like to acknowledge the help, constant guidance and support of Dr. Gabriel A. Elgavish, the head of the "Elgavish Lab" at the University of Alabama at Birmingham. He created a perfect atmosphere for learning and working in science and gave me invaluable advises to both academic and personal life.

I am grateful for the hard work of my immediate colleagues, Drs. Tamás Bodnár, Réka Faludi, Eszter Fődi, Róbert Kirschner, Pál Kiss, Zsófia Lenkey, Balázs Ruzsics, Pál Surányi and Levente Tóth, and I thank my former professor, Dr. Lajos Papp, as well as my current chief, Dr. Sándor Szabados for their continuing support.

I am thankful for the help of our collaborators, Drs. Brigitta C. Brott, Ada Elgavish, Satinder P. Singh, Dezhi Wang and the staff at the University of Alabama at Birmingham Animal Resources Program (Drs. Robert A. Baker, Eric D. Dohm, Cheryl R. Killingsworth, as well as Deidra H. Isbell).

I would also like to acknowledge the support from the National Institutes of Health, National Heart, Lung and Blood Institute for the following research grants that made this work possible: R41 HL-080886, R41 HL-084844.

Last but far not the least, I would like to thank my parents Éva and Gábor Varga-Szemes, as well as my wife and daughter, Évi and Dora, for their faithful support throughout the years.